

instability of a flattened disk, and nonlinear coupling with the large infall velocities associated with the accretion of the residual interstellar cloud.

Figure 3 shows the dependence of the pressure on the temperature in models A and B, compared to an arbitrary adiabat for a nebula composed of molecular hydrogen. The matter in model B is generally colder than that in A at a given pressure, because of the absence of the initial  $1.000 M_{\odot}$  proto-sun. The bar in model B is clearly hotter than the azimuthal average. Both models converge at high temperatures (late times), because at temperatures above  $\approx 1500$  K the dust opacity vanishes, molecular and atomic opacities are factors of  $\sim 100$  lower than dust opacities, and the nebula midplane becomes less optically thick locally, which acts as a thermostat on the midplane temperature.

These models have shown that compressional heating of infalling nebula gas may be sufficient to produce temperatures on the order of 1500 K in the inner solar nebula. Temperatures this high are intriguing, in light of meteoritic evidence for temperatures of 1500 K to 2000 K in the inner solar nebula. Peak temperatures of 1700 K are needed to melt Type B CAIs (18), and peak temperatures of 1700 K to 1900 K are required to melt chondrules (4). The evidence for rapid cooling of chondrules and Type B CAIs (time scales on the order of hours to days) may be difficult to reconcile with a globally hot inner solar nebula (4). However, because temperatures decrease quickly away from the midplane (falling to  $\sim 600$  K within 0.1 AU above or below the midplane), particles transported by convection to the nebula photosphere might be rapidly cooled (19). Also, the extra degree of freedom in a strongly nonaxisymmetric solar nebula may allow even more flexibility in scenarios for understanding meteorite formation. For example, if solid bodies in the nebula move relative to the gas at  $\sim 10^4$  cm s $^{-1}$  (20), and thus move relative to the nonaxisymmetric temperature distribution, it would be possible for particles to pass in or out of high temperature regions within a few hours if shocks of spatial extent no more than 1000 km exist. The present solar nebula models are quite incapable of resolving shock structure on such a small scale; deciding whether or not this scenario is possible must await future work.

#### REFERENCES AND NOTES

1. A. G. W. Cameron, *Icarus* 1, 13 (1962).
2. H. C. Lord III, *ibid.* 4, 279 (1965); J. W. Larimer, *Geochim. Cosmochim. Acta* 31, 1215 (1967); L. Grossman, *ibid.* 36, 597 (1972).

3. U. B. Marvin, J. A. Wood, J. S. Dickey, Jr., *Earth Planet. Sci. Lett.* 7, 346 (1970).
4. R. H. Hewins, in *Chondrules and Their Origin*, E. A. King, Ed. (Lunar and Planetary Institute, Houston, 1983), pp. 122–133.
5. R. B. Larson, *Mon. Not. R. Astron. Soc.* 145, 271 (1969).
6. A. G. W. Cameron and M. R. Pine, *Icarus* 18, 377 (1973).
7. A. G. W. Cameron, *Moon Planets* 18, 5 (1978); G. E. Morfill, in *Birth and Infancy of Stars*, R. Lucas, A. Omont, Eds. (North-Holland, Amsterdam, 1985), pp. 693–794; D. N. C. Lin and J. Papaloizou, in *Protostars and Planets II*, D. C. Black, M. S. Matthews, Eds. (Univ. of Arizona, Tucson, 1985), pp. 981–1072; A. G. W. Cameron, in *ibid.*, pp. 1073–1099.
8. W. Cabot et al., *Icarus* 69, 423 (1987).
9. J. A. Wood, *Earth Planet. Sci. Lett.* 70, 11 (1984); J. A. Wood, *Lunar Planet. Sci. Conf. XVII*, 956 (1986).
10. R. B. Larson, *Mon. Not. R. Astron. Soc.* 206, 197 (1984); A. P. Boss, *ibid.* 209, 543 (1984).
11. A. P. Boss, *Lunar Planet. Sci. Conf. XIX*, 122 (1988).
12. ———, *Astrophys. J.* 236, 619 (1980); *ibid.* 277, 768 (1984).
13. J. B. Pollack, C. P. McKay, B. M. Christofferson, *Icarus* 64, 471 (1985).
14. V. S. Safronov, *Evolution of the Protoplanetary Cloud and Formation of the Earth and Planets* (Nauka, Moscow, 1969) (translation NASA TTF-677, 1972).
15. J. S. Lewis, *Science* 186, 440 (1974).
16. A. P. Boss, G. E. Morfill, W. M. Tscharnuter, in *Planetary and Satellite Atmospheres: Origin and Evolution*, J. B. Pollack and S. K. Atreya, Eds. (Univ. of Arizona, Tucson, in press).
17. A. P. Boss, *Astrophys. J. Suppl.* 62, 519 (1986).
18. E. Stolper and J. M. Paque, *Geochim. Cosmochim. Acta* 50, 1785 (1986).
19. A. G. W. Cameron and M. B. Fegley, *Icarus* 52, 1 (1982).
20. S. J. Weidenschilling, *Mon. Not. R. Astron. Soc.* 180, 57 (1977).
21. I thank R. W. Carlson, D. D. Clayton, M. B. Fegley, L. Grossman, R. O. Pepin, F. Tera, J. T. Wasson, S. J. Weidenschilling, G. W. Wetherill, and J. A. Wood for encouraging discussions, J. A. Wood and G. E. Morfill for an instructive preprint, and A. G. W. Cameron and M. B. Fegley for comments on the manuscript. The calculations were performed on the Numerix NMX-432 array processor of the Carnegie Institution of Washington. Supported by the Innovative Research Program and the Planetary Geology and Geophysics Program of the National Aeronautics and Space Administration.

31 March 1988; accepted 24 May 1988

## A Tsunami Deposit at the Cretaceous-Tertiary Boundary in Texas

JOANNE BOURGEOIS, THOR A. HANSEN, PATRICIA L. WIBERG, ERLE G. KAUFFMAN

**At sites near the Brazos River, Texas, an iridium anomaly and the paleontologic Cretaceous-Tertiary boundary directly overlie a sandstone bed in which coarse-grained sandstone with large clasts of mudstone and reworked carbonate nodules grades upward to wave ripple-laminated, very fine grained sandstone. This bed is the only sandstone bed in a sequence of uppermost Cretaceous to lowermost Paleocene mudstone that records about 1 million years of quiet water deposition in midshelf to outer shelf depths. Conditions for depositing such a sandstone layer at these depths are most consistent with the occurrence of a tsunami about 50 to 100 meters high. The most likely source for such a tsunami at the Cretaceous-Tertiary boundary is a bolide-water impact.**

THERE IS CONSIDERABLE EVIDENCE for terrestrial impact by bolides throughout the Phanerozoic, including evidence for at least one at the Cretaceous-Tertiary (K-T) boundary [for counterarguments and references see (1)]. If the locations of such impacts were random, three to four tsunami-generating impacts in water should occur for every impact on land. Diagnostic evidence for these tsunamis is most likely to be preserved in strata deposited on the continental margin. Conformable sections of Upper Cretaceous to Paleocene continental-margin deposits around the Gulf of Mexico and in the western Atlantic contain coarse-grained beds at or close to the K-T boundary, and some unconformable sections contain breccias at the boundary (2–13, Fig. 1). We suggest that these coarse-grained beds may be tsunami deposits (14).

Some of these occurrences (Fig. 1) have

been attributed to the effects of a latest Cretaceous sea-level excursion (6–8, 15). Estimates for the magnitude of sea-level change near the K-T boundary range from negligible (3, 16) to more than 100 m (5, 17, 18); the age assigned to the postulated maximum low stand varies by several million years, from Late Cretaceous to early Paleocene (8, 17, 19). Many workers have suggested that sea level was high at the K-T boundary (2, 3, 18, 20), whereas others have suggested that a low stand coincided with the boundary (21).

We studied an unusual sandstone bed in midshelf to outer shelf mudstone at five

J. Bourgeois and P. L. Wiberg, Department of Geological Sciences, AJ-20, University of Washington, Seattle, WA 98195.

T. A. Hansen, Department of Geology, Western Washington University, Bellingham, WA 98225.  
E. G. Kauffman, Department of Geological Sciences, University of Colorado, Boulder, CO 80309.

well-exposed outcrops and in two cores in the vicinity of the Brazos River, Texas (Fig. 1). The K-T boundary section is conformable at the Brazos locality (Fig. 2) (2, 3, 21–24), and we do not see evidence of a significant sea-level change associated with the boundary section there; nor did Jiang and Gartner (3). The physical characteristics, biostratigraphy, magnetostratigraphy, and Ir content of the bed and bracketing mudstone are illustrated in Fig. 2 (21–24). Beneath the boundary section (Fig. 2) is more than 10 m of Upper Cretaceous shelf mud-

stone with no distinct sandstone layers; above is 1 to 4 m of similar mudstone of Paleocene age, capped by a condensed section, overlain by more mudstone (2).

The sandstone bed has an erosional base with up to 70 cm of local relief. The basal, coarse-grained sandstone is rich in shell fragments, glauconite and phosphate pellets, fish teeth, wood debris, rounded clasts of calcareous mudstone, and angular clasts of mudstone that are commonly >5 cm across (the largest observed is about 100 cm in the longest exposed dimension). This basal layer

grades upward through parallel-laminated and wave ripple-laminated (22), very fine grained sandstone, to siltstone (locally calcitized) and mudstone that are barren of macrofossils. Thin sections reveal that the sandstone contains up to about 20% redeposited foraminifera. At several exposures, the sandstone bed comprises two or more amalgamated graded beds; the total thickness ranges from about 30 to 130 cm (Fig. 1).

The Cretaceous and Paleocene molluscan macrofauna in mudstone directly below and above the sandstone bed indicate midshelf to outer shelf depths, and the fauna in the mudstone below it. Also, on the basis of benthic foraminiferal paleoecology, Sliter (25) estimated that the depth of deposition of the mudstone was 75 to 200 m. Furthermore, Jiang and Gartner (3) observed that the calcareous nannofossil assemblage was similar below, within, and for about 20 cm above the sandstone. In addition, there is no sedimentological evidence of inner shelf, shoreface, or brackish water conditions, which likely would have occurred in a backstepping shelf sequence, transgressive lag deposit, or estuarine fill of a ravinement. Because the Brazos sites are about 100 km away from the latest Cretaceous shelf edge (26), and because shallower depth estimates are a more critical test of our interpretation that the coarse bed is a tsunami deposit, we have used water depths of 50 and 100 m for calculating the conditions needed to deposit the sandstone bed (27).

Deposition of the sandstone bed requires (i) initial shear velocities on the order of 15 to 100 cm/s to erode and transport the mud clasts (28) and (ii) a rapid drop in the shear velocities to less than 1 cm/sec, under oscillatory flow conditions, to form wave ripples in the very fine sand (29). Only a tsunami is likely to have produced these conditions on the continental shelf. Winnowing and erosion, as can happen on continental shelves when sea level drops and then rises, would not have produced graded bedding or climbing ripples. A turbidity current (30) would have produced asymmetric rather than symmetric ripples. A storm could not have moved mud clasts of the size observed in 50 to 100 m of water (Table 1). Moreover, other sandstone beds should punctuate the Cretaceous and Paleogene mudstone sequence if the sandstone bed at the K-T boundary were the product of a normal (that is, common) turbidity current, or of a storm, or if the water depth were shallower (31).

We propose that a very large tsunami (>50-m wave height) caused major erosion at the shelf break and on the shelf, transport-

**Fig. 1.** Some K-T boundary sites of interest to this study (not all-inclusive). Closed circles are conformable K-T sections with coarse-grained deposits at or near the boundary (? indicates inconclusive or incomplete biostratigraphic analysis), open circles are sections with a disconformable K-T boundary; Littig Pit and Walker Creek inner-shelf(?) localities in Texas (a) are missing uppermost K and lowermost T; a condensed section lies at the boundary (2, 3); Kauffman and Hansen (4) have noted that a bed of large chaotic blocks occurs directly below the K-T boundary(?) in inner-shelf sedimentary rocks in the Paoras and La Popa basins of northern Mexico and near Eagle Pass, Texas (b); at a terrestrial site in Arkansas (c), a chaotic boulder bed has been attributed to a tsunami (5); coarse-grained beds in a shallow marine section at Braggas, Alabama (d), have been interpreted to indicate sea-level change of at least tens of meters (6–8); continental slope and rise sections (e) (DSDP sites 605 and 603) contain a sand layer at the boundary that has been tentatively attributed to a tsunami (9); a “major volcanogenic turbidite layer” occurs at the boundary at (f) (10); an intraformational breccia is present at the boundary at (g), DSDP site 153 (11); unconformable boundaries occur at DSDP sites 95 and 97 (h) with no event beds (12). Borella (13) noted turbidities and debris and slump breccias at the boundary in a southeast section Atlantic (off the map); he tentatively attributed them to intense tectonic activity.

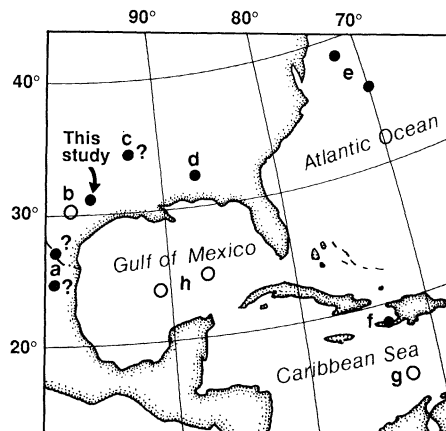


**Fig. 2.** Detailed measured sections of the K-T boundary section at Brazos 1 and two exposures within 3 km of Brazos 1 (2); correlation is on the basis of lithology; DMC, Darting Minnow Creek; CMC, Cottonmouth Creek; the width of the section represents grain size; M, mudstone; FS, fine sand; CS, coarse sand; lithologic symbols are (a) shell debris; (b) sand; (c) mudstone; (d) calcareous cement or replacement; (e) wave-ripple lamination, not hummocky cross-stratification (22); and (f) parallel lamination. Iridium (23) and faunal analyses are from Brazos 1 except for (k) and (m), which are a generalized representation; symbols are (g) magnetostratigraphy (23) (from a Brazos core); (h) schematic representation of *Prediscosphaera quadripunctata* acme zone of the *Micula murus* zone (extends beyond the base of the represented section) (3); (i) first appearance of *Globoconusa conusa* (zone Pob) (24); (j) bloom of *Thoracosphaera* sp. (3); (k) (schematic) typical Cretaceous molluscan fauna decrease in number of species in sandstone bed, which marks their last appearance at Brazos sites; (m) first appearance of Paleocene mollusks, *Bittium estellense* (Aldrich) and *Calyptrophorus* c.f. *aldrichi* (Gardner), 20 to 30 cm above top of wave-rippled bed. The paleontologic K-T boundary is typically located by (i) and (j).

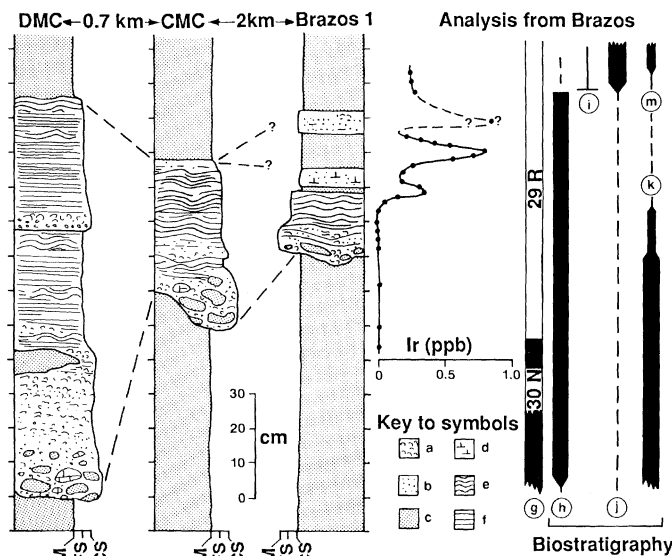


**Table 1.** Calculated shear velocities ( $U_*$ , in centimeters per second) in water depths of 50 and 100 m for wind-generated storm waves of period  $T$  (39); wavelength  $L$ , not specified, ranges from 100 to 520 m. A characteristic roughness of 1 cm was used. Sediment-transport calculations indicate that a *minimum*  $U_*$  of 15 cm/s is necessary for transporting typical clasts in the sandstone bed, and a  $U_*$  as high as 100 cm/s may be required to move the largest clast observed (28).

$T$ (min)	Shear velocity (cm/s) for wave heights of						
	2 m	4 m	6 m	8 m	10 m	15 m	20 m
<i>Water depth = 50 m</i>							
8	*	1.4	1.9	2.4	†	†	†
12	2.1	3.8	5.4	7.0	8.5	12.1	†
16	2.7	4.9	6.9	8.9	10.9‡	(15.5)§	(20.0)
20	2.9	5.3	7.6	9.8	(11.9)	(17.0)	(21.9)
<i>Water depth = 100 m</i>							
8	*	*	*	*	*	†	†
12	*	1.2	1.7	2.3	2.7	3.3	4.9
16	1.4	2.5	3.5	4.5	5.5‡	(7.9)	(10.1)
20	1.8	3.2	4.5	5.9	(7.2)	(10.2)	(13.1)

\*Subcritical (no transport). †Wave too steep, will collapse. ‡Maximum recorded wave at 42.0°N, 125.0°W (eastern Pacific) from 1951 to 1974, from once-daily records. §Parentheses indicate extreme wave conditions, unlikely to occur except, possibly, for single waves.

**Table 2.** Calculated shear velocities ( $U_*$ , in centimeters per second) for tsunamis of varying wave height ( $H$ ), with periods ( $T$ ) of 30 and 60 min (37), at water depths ( $h$ ) of 50 and 100 m. Because a tsunami behaves everywhere as a shallow water wave, its wave speed  $C$  equals  $(gh)^{1/2}$ ; therefore, if the period  $T$  is specified, the wavelength  $L$  can be calculated ( $L = CT$ ).

$H$ (m)	Shear velocity (cm/s) for water depths of	
	50 m	100 m
<i>T = 30 min</i>		
1	0.6*	0.8*
10	4.7	6.2
50	21†	27
100	‡	52†
<i>T = 60 min</i>		
1	1.0	1.4
10	8.3	11.3
50	37†	50
100	‡	96†

\*Subcritical (no transport). †Wave boundary layer is thicker than water depth; also, wave is likely to break because  $H = h$ . ‡Cannot occur because  $H \gg h$ .

ed and redeposited shelf sediments, and concentrated older lag material such as bored limestone clasts and glauconite. The very fine sand may have been advected from the inner shelf, either by wave reflection or across imposed density gradients; however, the abundance of foraminifera in the sandstone and the absence of shallow water fauna indicate that the sand, if from the inner shelf, was mixed with more locally derived sediments. Individual graded layers could be produced by multiple waves—typical of known tsunamis—or by wave reflection. We estimate that the graded sandstone was deposited in about 1 day. The overlying 20 to 30 cm of mudstone could have been deposited within a few weeks of the initiating event, or longer (32); the absence of macrofauna in this mudstone suggests that it was also deposited rapidly.

Iridium fallout from a bolide impact would be concentrated in the more slowly deposited mudstone intervals rather than in the sandstone (Fig. 2). We do not attach great significance to the number of Ir peaks (Fig. 2), but they may be attributed to this grain-size variation.

Tsunamis, which are impulse-generated wave trains, can result from earthquakes, explosive volcanism, submarine landslides, and bolide-water impacts; all of these mechanisms apparently produce tsunamis with similar wave periods ( $10^1$  min) and wavelengths ( $10^2$  km) (33–35). Although most tsunamis have initial wave heights of meters to tens of meters, wave heights of 100 m or more have been observed or postulated for tsunamis generated by volcanic eruptions and prehistoric submarine landslides (34, 35). Initial wave heights for bolide-water impacts depend on bolide radius, water depth, and other factors such as atmospheric pressure (36); for large bolide (radii of kilometers) impacts, tsunamis may be as high as the water depth of the impact site, that is, on the order of 4 to 5 km for a deep ocean impact. Wave heights decrease as the tsunami spreads radially; only a bolide-water impact can produce a far-field wave height in the range of 10 to 100 m (36).

Simple calculations (37) (Table 2) show that for shelf depths of 50 to 100 m and a tsunami of ordinary period and wavelength, only a wave on the order of 50 to 100 m high can produce the conditions necessary for erosion of the mud clasts and deposition of the sandstone bed at the Brazos sites. Generation of such wave heights probably requires a nearby volcanic explosion on the scale of Krakatau or larger, a nearby submarine landslide also of great size, or a bolide-water impact in the ocean. A 10-km-diameter bolide could hit the deep ocean up to

about 5000 km away and produce the required conditions (36); a more proximal impact in shallower water or of a smaller object could also produce the tsunami. If nearby explosive volcanism produced the tsunami, a distinctive ash layer should be preserved above the sandstone bed or in Caribbean or Atlantic deep-sea cores; such a layer has not been reported (38). If the tsunami were produced by a major submarine landslide, it should not occur precisely at the K-T boundary unless the landslide were caused by an earthquake related to boundary events, which is a possibility. A number of scenarios of bolide-water impacts, from a large impact in deep water far away from the Brazos site to a smaller impact in shallow water in the west-central Atlantic or closer, could generate the specified conditions.

#### REFERENCES AND NOTES

1. A. Hallam, *Science* **238**, 1237 (1987).
2. T. Hansen *et al.*, *Cretaceous Res.* **8**, 229 (1987).
3. M. J. Jiang and S. Gartner, *Micropaleontology* **32**, 232 (1986).
4. E. G. Kauffman and T. A. Hansen, *II World Basque Conference, Paleontology and Evolution: Extinction Events* (abstr.) (University del Pais Vasco, Leioa, Spain, 1987), p. 28.
5. E. E. Glick, *Geol. Soc. Am. Abstr.* **16**, 85 (1984); C. G. Stone, *ibid.*, p. 115.
6. A. D. Donovan and P. R. Vail, *ibid.* **18**, 587 (1986); J. Reinhardt, J. S. Schindler, A. D. Donovan, *ibid.*, p. 728; Reinhardt *et al.* discussed disconformities in the eastern Gulf Coast; see also J. Reinhardt, Ed., *Stratigraphy and Sedimentology of Continental, Near-shore, and Marine Cretaceous Sediments of the Eastern Gulf Coastal Plain* (Society of Economic Paleontologists and Mineralogists—American Association of Petroleum Geologists, Field Trip 3, Tulsa, 1986).
7. A. D. Donovan *et al.*, in *Sea-Level Change—an Integrated Approach*, C. Wilgus *et al.*, Eds., *Soc. Econ. Paleontol. Mineral. Spec. Publ.*, in press.
8. D. S. Jones *et al.*, *Geology* **15**, 311 (1987).
9. J. E. Van Hinte *et al.*, *ibid.* **13**, 392 (1985); J. E. Van Hinte *et al.*, *ibid.*, p. 397.
10. J.-M. R. Maurrasse, *Geol. Soc. Am. Abstr.* **18**, 686 (1986).
11. I. Premoli-Silva and H. M. Bolli, *Init. Rep. Deep Sea Drill. Proj.* **15**, 499 (1975).
12. B. W. McNeely, *ibid.* **10**, 679 (1973).
13. P. E. Borella, *ibid.* **74**, 645 (1984).
14. See also the legend to Fig. 1, especially discussion of locations (c) and (e), and (5, 9).
15. Hallam (1) interprets sites at (c) (Fig. 1) as representing a sea-level low stand during the latest Cretaceous.
16. See Jones *et al.* (8) for an intermediate view.
17. Hallam (1) summarized several sea-level curves.
18. B. U. Haq, J. Hardenbol, P. R. Vail, *Science* **235**, 1156 (1987).
19. Compare sea-level curves in (7) and (18); Hansen *et al.* (2) summarized evidence for an early Paleocene low stand.
20. Also suggested by fine mudstone at the K-T boundary with slowest rates of sedimentation at Deep-Sea Drilling Project (DSDP) site 603 (9).
21. For example, Hallam (1); suggested by Donovan *et al.*, (7).
22. The typical ripple wavelength is 15 cm; ripples are regular; Hansen *et al.* (2) mistakenly referred to this structure as hummocky cross-stratification.
23. Iridium analyses from F. Asaro *et al.*, in *Texas Ostracoda*, R. F. Maddocks, Ed. (University of Houston, Houston, Texas, 1982), pp. 238–241; magnetostratigraphy from W. Gose, personal communication.
24. G. Keller, personal communication.
25. W. V. Sliter, personal communication.

26. C. D. Winker, *Gulf Coast Section Soc. of Econ. Paleontol. Mineral. 5th Annual Research Conference* Austin, TX (1982), p. 109.
27. In depths shallower than about 50 m, we would expect to see more evidence of wave activity; in depths >100 m, the coarse bed would be even more remarkable.
28. We estimated the shear velocity ( $U_s$ ) necessary to erode and transport a clast 20 by 100 cm in cross section (in the DMC section, Fig. 2) by calculating the force necessary to push this block across the bed; with a clast density of 2.0 g/cm<sup>3</sup> and a coefficient of static friction of 0.5, the necessary  $U_s$  is 35 to 100 cm/s, depending on how much the clast is projecting above the surface. The  $U_s$  necessary to initiate motion of typical clasts (5 to 20 cm diameter) in the basal sandstone, over a rough bed (1 cm characteristic roughness), is at least 15 cm/s, which can be used as a minimum requirement [method of P. L. Wiberg and J. D. Smith, *Water Resour. Res.* 23, 1471 (1987)]; a shear velocity of about 25 cm/s and a wave period of 50 min are sufficient to suspend enough sand to form a 20-cm-thick sand layer with climbing ripples; sediment concentration profiles calculated after J. D. Smith [in *The Sea*, E. D. Goldberg, Ed. (Wiley, New York, 1977), vol. 6, pp. 539–577]; P. L. Wiberg and J. D. Smith, *Continental Shelf Res.* 2, 147 (1983).
29. This size of sediment (about 0.06-mm diameter) goes directly into suspension when the critical shear stress is exceeded. Therefore, the wave ripples must be generated by deposition under an oscillatory velocity field with a subcritical shear stress (Table 1). For wave ripples of 15-cm wavelength (22) to form, the minimum wave height to produce the appropriate orbital diameter in 50-m water depth is 1 m for 10-s waves or 3 m for 8-s waves; in 100-m water depth 2 m for 12-s waves or 6 m for 10-s waves [technique of P. L. Wiberg and J. Bourgeois, *Soc. Econ. Paleontol. Mineral. Annual Midyear Mtg. Abstr.* 3, 116 (1986); see also H. E. Clifton and J. R. Dingler, *Mar. Geol.* 60, 165 (1984)]. Thus the occurrence of these ripples is indicative of waves with long period and low wave height.
30. By turbidity current, we mean a normal, discrete, sediment-laden current flowing along the bed, which would produce unidirectional current indicators. The turbulence generated by a tsunami of the scale postulated would suspend enough sediment to produce density gradients in the water column, which would cause sediment advection, for example, of sandy sediment from close to shore toward the site of deposition.
31. Large storm waves could generate shear stresses of the magnitude necessary to produce the bed only if the environment were shallow, about 10- to 20-m water depth; if this were the case, other evidence of storm waves would be present in the 12 m of bracketing mudstone (which would likely have several sandy intervals and would be coarser).
32. After initial turbulence, the sand (settling velocity of about 0.25 cm/s) would settle out of 100 m of water in about 12 hours; the silt and clay would take a few days to settle out, depending on the residual turbulence.
33. See, for example, R. A. Heath and M. M. Creswell, Eds., *Tsunami Research Symposium 1974* (Unesco Press, Paris, 1974); K. Iida and T. Iwasaki, Eds., *Tsunamis: Their Science and Engineering* (Reidel, Dordrecht, 1981); for a review of the scale of submarine slides, see D. G. Moore, in *Rocksides and Avalanches*, vol. 1, *Natural Phenomena*, B. Voight, Ed. (Elsevier, Amsterdam, 1978), pp. 563–604.
34. F. M. Bullard, *Volcanoes of the Earth* (University of Texas, Austin, 1984); T. Simkin and R. S. Fiske, Eds., *Krakatau, 1883—The Volcanic Eruption and Its Effects* (Smithsonian Institution, Washington, DC, 1983).
35. G. W. Moore and J. G. Moore, *Geol. Soc. Am. Abstr.* 17, 668 (1985).
36. The effects of tsunamis generated by impacts are reviewed by D. E. Gault and C. P. Sonett, *Geol. Soc. Am. Spec. Pap.* 190, 69 (1982).
37. These calculations are meant to indicate only order-of-magnitude conditions; no theory is established for the behavior of large tsunamis, particularly in shelf depths.
38. But see Maurrasse (10) and Borella (13).

39. In the present Gulf of Mexico, typical fair-weather wave periods are 3 to 6 s; storms produce waves with periods of 8 to 10 s. Differing paleogeography, that is, greater fetch, could produce larger waves, as in the modern Pacific, which has the largest measured waves.
40. We thank W. Gose, G. Keller, and W. V. Sliter for sharing unpublished data; J. D. Smith for discussions about waves and sediment-transport calcula-

tions; B. Atwater for reviewing an early version of this manuscript; and A. D. Donovan and J. Reinhardt for sharing information about the Braggs, Alabama, locality. This research was supported in part by donors to the Petroleum Research Fund of the American Chemical Society (to J.B.) and NSF grant EAR-8411202 (to T.A.H. and E.G.K.).

23 May 1988; accepted 6 July 1988

## DNAs of the Two Mating-Type Alleles of *Neurospora crassa* Are Highly Dissimilar

N. LOUISE GLASS, STEVEN J. VOLLMER,\* CHUCK STABEN, JEFF GROTELUESCHEN, ROBERT L. METZENBERG, CHARLES YANOFSKY

The mating-type alleles *A* and *a* of *Neurospora crassa* control mating in the sexual cycle and function in establishing heterokaryon incompatibility in the vegetative cycle. The *A* and *a* alleles were cloned, and they were shown to encode both the sexual functions and vegetative incompatibility. The mating-type clones contain nonhomologous DNA segments that are flanked by common DNA sequences. *Neurospora crassa* and all heterothallic and pseudohomothallic *Neurospora* species contain a single copy of one mating-type sequence or the other within each haploid genome. The six known self-fertile homothallic isolates contain an *A* homolog, but only one species also contains a homologous sequences. Homothallism in these species is not due to mating-type switching, as it is in *Saccharomyces cerevisiae*.

**N**EUROSPORA CRASSA IS A HAPLOID heterothallic filamentous fungus; its two mating types are designated *A* and *a* (1, 2). Fusion of cells of opposite mating type initiates a series of developmental events leading to the formation of a fruiting body (perithecium) containing many asci, each with ascospores that bear the haploid products of meiosis. There is no visible difference between strains of the two

mating types, and otherwise nearly isogenic strains will mate provided that they are of

N. L. Glass, J. Grotelueschen, R. L. Metzzenberg, Department of Physiological Chemistry, University of Wisconsin, Madison, WI 53706.  
S. J. Vollmer, C. Staben, C. Yanofsky, Department of Biological Sciences, Stanford University, Stanford, CA 94305.

\*Present address: CODON, 213 East Grand Avenue, South San Francisco, CA 94080.

**Fig. 1.** Transformation of *a*<sup>m1</sup>, *ad-3B*, *cyh-1* (FGSC 4564) (8) spheroplasts (6) by pSV50 and pSV6:10A. DNA (2.5 μg) of pSV50 (encoding an altered β-tubulin that confers resistance to benomyl) (6, 9) or pSV6:10A (encoding both altered β-tubulin and *A* mating-type function) were introduced by transformation. Transformation plates containing 0.5 μg/ml benomyl were incubated at 30°C for 4 days after plating. Whatman 1 filter paper was placed on the agar surface, and transformants were allowed to grow into the filters for 12 hours. The filters were then transferred to plates containing an *a* mating-type tester inoculated 4 days previously with the highly fertile nonconidiating strain *fl*<sup>P</sup>*a* (FGSC 4347). The plates were incubated at 25°C for 4 days. Transformants carrying pSV6:10A express the *A* mating-type function and induce the formation of black perithecia in the *fl*<sup>P</sup>*a* lawn. The location of the mating-type *A* function was determined by transformation of *a*<sup>m1</sup> spheroplasts with restriction fragments of pSV6:10A. Cosmid pSV6:10A was digested with various restriction enzymes and the digests were used in conjunction with the benomyl resistance vector, pSV50, to cotransform the *a*<sup>m1</sup> recipient. Previous studies demonstrated that approximately 80% of transformed *Neurospora* spheroplasts are cotransformed when two separate DNA fragments are used simultaneously; a selectable marker is necessary in only one of the fragments (6). Benomyl-resistant transformants that receive a functionally intact *A* gene (that is, one not disrupted by cleavage with a restriction enzyme) initiate perithecium development when crossed to *a* mating-type protoperithecia. Restriction fragments that induced perithecium development were subcloned into pGem vectors (Promega Biotec, Inc.).

